



# Examining the sensitivity of $^{18}\text{F}$ -NaF PET for the imaging of cardiac amyloidosis

Patrick Martineau, MD, PhD,<sup>a,b</sup> Vincent Finnerty, MSc,<sup>c</sup> Geneviève Giraldeau, MD,<sup>d</sup> Sébastien Authier, B Eng,<sup>c</sup> Francois Harel, MD, PhD,<sup>c</sup> and Matthieu Pelletier-Galarneau, MD, MSc<sup>b,c</sup>

<sup>a</sup> Department of Radiology, Health Sciences Centre, University of Manitoba, Winnipeg, MB, Canada

<sup>b</sup> Gordon Center for Medical Imaging, Massachusetts General Hospital, Harvard University, Boston, MA

<sup>c</sup> Department of Medical Imaging, Institut de Cardiologie de Montréal, Montreal, QC, Canada

<sup>d</sup> Department of Medicine, Institut de Cardiologie de Montréal, Montréal, Canada

Received Dec 14, 2018; accepted Feb 21, 2019

doi:10.1007/s12350-019-01675-2

**Background.** Conventional nuclear imaging with bone-seeking radiopharmaceuticals has been shown to be a sensitive test for the detection of transthyretin cardiac amyloidosis (ATTR); however, to date, few data exist on the utility of  $^{18}\text{F}$ -sodium fluoride (NaF) positron emission tomography (PET) in subjects with cardiac amyloidosis (CA).

**Methods.** Myocardial perfusion imaging and cardiac  $^{18}\text{F}$ -NaF PET/CT of 7 subjects with ATTR, four with light-chain CA (AL), and four controls were retrospectively reviewed. Qualitative interpretation and quantitative analyses with average left ventricular standardized uptake values ( $\text{SUV}_{\text{mean}}$ ) and target-to-background ratios ( $\text{TBR}_{\text{mean}}$ ) were performed.

**Results.** Average  $\text{TBR}_{\text{mean}}$  was significantly increased in subjects with ATTR ( $0.98 \pm 0.09$ ) compared to AL ( $0.85 \pm 0.08$ ,  $P = .026$ ) and CTL ( $0.82 \pm 0.07$ ,  $P = .020$ ), while  $\text{SUV}_{\text{mean}}$  was not ( $P = .14$ ). Receiver-operator characteristic (ROC) analysis yielded an area under the curve (AUC) of 0.91, with a sensitivity/specificity of 75%/100% for  $\text{TBR}_{\text{mean}}$  using a cutoff value of 0.89 for the diagnosis of ATTR. Qualitative interpretation resulted in a sensitivity/specificity of 57%/100% for ATTR.

**Conclusions.** While  $^{18}\text{F}$ -NaF PET/CT demonstrates good diagnostic accuracy for ATTR, particularly when using quantitative analysis, the low  $\text{TBR}_{\text{mean}}$  values observed in ATTR indicate poor myocardial signal.  $^{18}\text{F}$ -NaF PET/CT is not yet ready for clinical use in CA until further comparison studies are performed with  $^{99\text{m}}\text{Tc}$ -DPD/PYP. (J Nucl Cardiol 2021;28:209–18.)

**Key Words:** Cardiac amyloidosis • transthyretin • ATTR • bone scintigraphy • sodium fluoride • positron emission tomography

**Electronic supplementary material** The online version of this article (<https://doi.org/10.1007/s12350-019-01675-2>) contains supplementary material, which is available to authorized users.

The authors of this article have provided a PowerPoint file, available for download at SpringerLink, which summarises the contents of the paper and is free for re-use at meetings and presentations. Search for the article DOI on SpringerLink.com.

Reprint requests: Matthieu Pelletier-Galarneau, MD, MSc, Department of Medical Imaging, Institut de Cardiologie de Montréal, 5000 Belanger, Montreal, Quebec, H1T1C8, Canada; [mattgalarneau@gmail.com](mailto:mattgalarneau@gmail.com)

1071-3581/\$34.00

Copyright © 2019 American Society of Nuclear Cardiology.

### Abbreviations

AL	Light-chain amyloidosis
ATTR	Transthyretin cardiac amyloidosis
CA	Cardiac amyloidosis
cMRI	Contrast enhanced magnetic resonance imaging
DPD	Diphosphonopropanodicarboxylic acid
EMB	Endomyocardial biopsy
LVH	Left ventricular hypertrophy
MDP	Methylene diphosphonate
NaF	Sodium fluoride
PYP	Pyrophosphate
SUV	Standard uptake value
TBR	Target-to-background ratio

**See related editorial, pp. 219–224**

## INTRODUCTION

Cardiac amyloidosis (CA) consists of a group of diseases, each characterized by the deposition of insoluble, misfolded proteins in the myocardium.<sup>1</sup> CA is classified based on the type of protein accumulating in the heart with two main recognized subtypes: light-chain (AL) CA and transthyretin CA (ATTR).<sup>2</sup> Classically, CA presents with diastolic dysfunction and left ventricular hypertrophy (LVH) secondary to accumulation of proteins in the myocardium.<sup>3</sup> It has been proposed that CA is responsible for a significant proportion of patients presenting with heart failure with preserved ejection fraction or with LVH.<sup>4,5</sup> Increased recognition of CA and a growing interest in developing new diagnostic tools have been observed over the past few years, in part due to the development of new treatments such as tafamidis (*Vyndaquel*) and patisiran (*Onpattro*) for ATTR.<sup>6,7</sup>

Although definitive diagnosis of CA has traditionally been established through endomyocardial biopsy (EMB), a large multicentric study has recently demonstrated that EMB can be avoided in a significant number of patients with the use of bone scintigraphy with <sup>99m</sup>Tc-PYP or <sup>99m</sup>Tc-DPD.<sup>8</sup> Indeed, molecular imaging with these bone agents has a near-perfect sensitivity (> 99%) for the detection of ATTR.<sup>8</sup> Furthermore, it was shown that scintigraphy could reliably distinguish between AL and ATTR, as uptake is highly selective for ATTR.<sup>8–11</sup> This distinction is crucial as the management and outcome of patients AL and ATTR differ significantly.

Recently, there has been growing interest in using <sup>18</sup>F-sodium fluoride (<sup>18</sup>F-NaF) for the diagnosis of ATTR.<sup>12–15</sup> Unlike the other bone-seeking agents

traditionally used for ATTR, <sup>18</sup>F-NaF is a positron emission tomography (PET) tracer, which offers improved imaging properties compared to <sup>99m</sup>Tc-based tracers, as well as allowing for accurate quantification. These features could potentially lead to enhanced diagnostic performance, especially at the early stages of the disease; however, it has been established that the diagnostic performance of the various bone-seeking radiopharmaceuticals are not all equivalent thus necessitating an assessment of the diagnostic performance of <sup>18</sup>F-NaF for this application.<sup>16</sup> The purpose of this study is to examine the role of <sup>18</sup>F-NaF imaging in the diagnosis of ATTR.

## METHODS

### Patient Cohort

This retrospective study was approved by our institutional review board, and the requirement to obtain informed consent was waived. Medical records of subjects who underwent a <sup>18</sup>F-NaF PET/CT study for assessment of CA between October 2017 and September 2018 at the Institut de Cardiologie de Montréal were reviewed. All subjects also underwent same day rest perfusion imaging with either <sup>82</sup>Rb-PET/CT or <sup>99m</sup>Tc-tetrofosmin SPECT/CT. Rest perfusion imaging was systematically performed in all subjects undergoing <sup>18</sup>F-NaF PET/CT study for assessment of CA. These images were used to provide myocardial contours for quantitative analyses, as described below. Subjects who underwent <sup>18</sup>F-NaF PET/CT along with a perfusion study within 30 days for reasons other than CA evaluation were also included as controls. Subjects with incomplete studies were excluded.

### PET/CT Acquisitions

PET/CT scans were performed on hybrid 3D PET/CT scanner (Siemens Biograph mCT Flow 40 with TrueV or Siemens Biograph mCT Flow Edge with TrueV, Knoxville, TN, USA). For <sup>18</sup>F-NaF imaging, dynamic cardiac acquisition of 30 minutes was performed, 60 minutes following injection of approximately 370 MBq of <sup>18</sup>F-NaF. A low-dose CT for attenuation correction was acquired following NaF acquisition. For subjects who underwent resting imaging with <sup>82</sup>Rb PET/CT, imaging was performed on the same scanners with a 6 min PET acquisition using a 30 seconds infusion of 10 MBq/kg (RUBY-FILL, Jubilant DRAXIMAGE Inc., Kirkland, Québec, Canada). Another low-dose CT for attenuation correction was acquired following rest perfusion imaging. Global rest myocardial blood flow (MBF) values were quantitated using Corridor4DM (INVIA Medical Imaging Solutions, Ann Arbor, Michigan, USA), which relies on one-tissue-compartment model with flow-dependent extraction correction.<sup>17</sup>

## **<sup>18</sup>F-NaF PET/CT Interpretation**

Images were reviewed independently by two certified nuclear medicine specialists (FH and MPG), blinded to all clinical information, using syngo.via VB30 software (Siemens Healthcare, Germany). Disagreements were resolved by consensus. To perform quantitative analyses, LV segmentation was first performed on the rest perfusion images in order to define the LV contours. After registering the individual CTs performed on the corresponding perfusion and <sup>18</sup>F-NaF studies, the segmentation performed on the rest perfusion image was applied on the <sup>18</sup>F-NaF PET/CT study in order to define matching LV contours. Regions were manually repositioned to exclude uptake from the sternum or from valve calcifications (Figure 1). This method allowed for accurate segmentation of the LV on the <sup>18</sup>F-NaF PET/CT studies as segmentation based on the <sup>18</sup>F-NaF uptake proved to be inadequate in most cases due to the low myocardial uptake. A second region of interest was positioned in the LV cavity to estimate blood pool activity. Average standard uptake values (SUV<sub>mean</sub>) and target-to-background ratio (TBR<sub>mean</sub>) were extracted for the whole LV and for each myocardial segment. TBR<sub>mean</sub> was calculated by dividing myocardial SUV<sub>mean</sub> by blood SUV<sub>mean</sub>.

## **Gold Standard**

The gold standard consisted of biopsy results or, when unavailable, final clinical diagnosis of ATTR was obtained by following the nonbiopsy algorithm which relies on the results of bone scintigraphy and serum protein electrophoresis (SPEP).<sup>8</sup>

## **Statistical Analysis**

Continuous variables are presented as mean ± standard deviation (SD) and categorical variables as frequencies. Categorical variables were compared using Fisher's exact test. Continuous variables were compared with Student's two sample *t* test. When comparing multiple means, a one-way ANOVA was performed followed by the Holm-Sidak test. All statistical analyses were two-tailed, and a *P* value of < .05 was considered significant. All analyses were performed using GraphPad Prism (GraphPad Prism version 7.0 for Windows, GraphPad Software, California, USA).

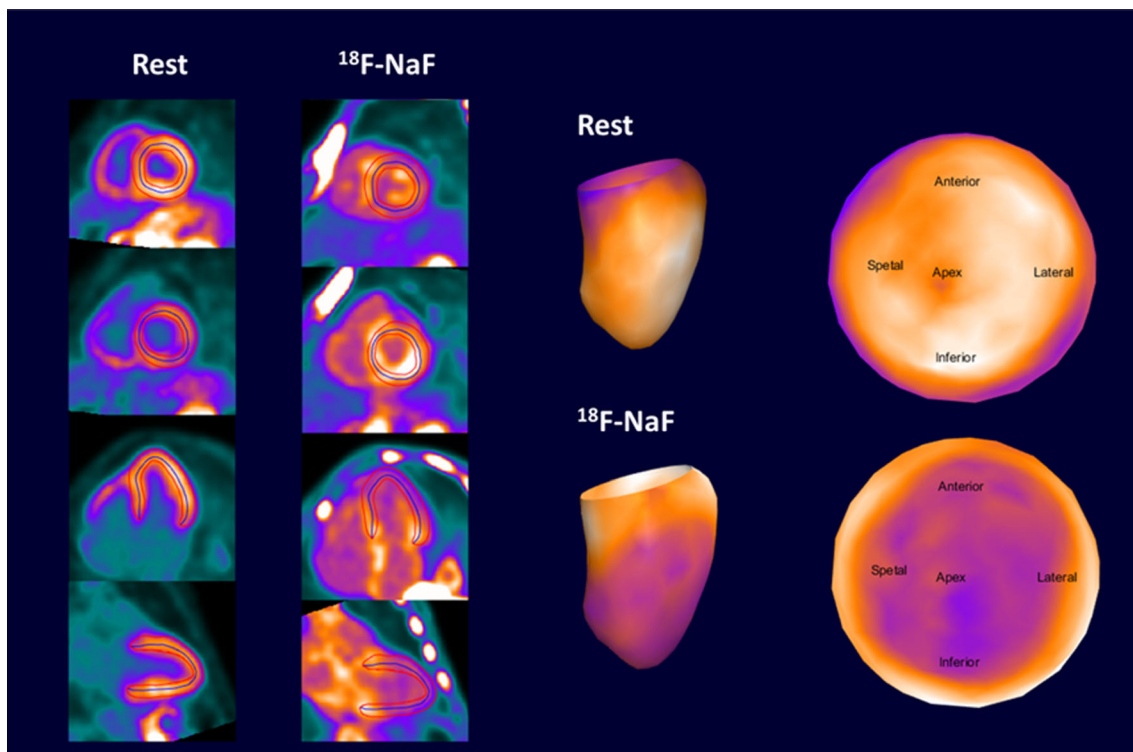


**Figure 1.** Example of the algorithm used to segment the left ventricle (LV) on the <sup>18</sup>F-NaF PET/CT images. The LV contours drawn on the rest perfusion study were transferred to the <sup>18</sup>F-NaF PET/CT studies using the CTs of both acquisitions as the registration reference. The region of interest was then manually repositioned to exclude areas of nonmyocardial uptake. In this example, the <sup>18</sup>F-NaF PET/CT images demonstrate increased uptake in the basal segments of the LV as well as in the atria and right ventricular free wall.

**Table 1.** Subjects' characteristics

	ATTR							AL				
	1	2	3	4	5*	6*	7*	1	2	3	4	
Age (year)	82	77	83	78	80	65	70	81	63	59	43	
Sex	M	M	M	M	M	M	M	M	F	M	F	
Ethnicity	C	C	C	C	C	C	C	H	C	C	C	
BMI (kg/m <sup>2</sup> )	25.7	28.2	24.2	26.0	23.5	27.5	22.1	24.5	24.5	23.1	27.8	
NYHA class	3	2	2	3	2	1	1	1	1	2	3	
Comorbidities												
HTA	No	No	Yes	No	Yes	Yes	Yes	Yes	No	No	No	
DLP	Yes	Yes	Yes	No	Yes	Yes	Yes	Yes	No	Yes	No	
CAD	No	Yes	No	Yes	No	No	No	Yes	No	No	No	
Diabetes	No	No	No	No	No	Yes	No	No	No	No	No	
Laboratories												
Troponin (ng/L)	150	-	56	40	30	39	29	23	32.2	127	128	
NTproBNP (ng/L)	6664	1334	1631	-	2231	651	2469	407	-	23571	4881	
Calcium (mmol/L)	-	-	-	-	2.15	2.38	2.1	-	2.16			
Creatinine (μmol/L)	151	88	80	104	150	99	98	92	49	148	75	
eGFR (mL/min/1.73 m <sup>2</sup> )	39	> 60	> 60	> 60	39	> 60	> 60	> 60	> 60	42	> 60	
Kappa (mg/L)	46.7	52.3	38	43	42.6	51.5	38	51.4	29	39.1	48.5	
Lambda (mg/L)	19	22.3	72.3	23.6	21.1	13.4	13.3	20.1		27.8	10.5	
Kappa:Lambda Ratio	11.6	15.3	49.5	18.2	20	16.2	7.7	13.1		136	950	
ECG												
Low Voltage	No	No	No	No	No	No	No	No	No	No	No	
LVH	Yes	No	No	No	Yes	Yes	No	Yes	No	Yes	No	
QRS (ms)	122	162	178	146	116	116	82	106	86	94	90	
Echo												
LVEF (%)	45	40	55	55	38	55	55	65	60	55	50	
LV mass (g/m <sup>2</sup> )	143	164	214	152	183	174	102	126	73	155	136	
Septum width (mm)	15	15	17	16	12	16	15	17	11	19	17	
E/e'	29	-	24	11	5	12	12	9	-	22	-	
Global strain (%)	-	- 12.8	-	- 8.8	-	- 13	- 12.5	-	-	-	-	
cMRI												
LGE	Yes	Yes	Yes	Yes	-	Yes	Yes	Yes	Yes	Yes	Yes	
Heterogeneous T1 nulling	Yes	Yes	Yes	Yes	-	Yes	Yes	Yes	Yes	Yes	Yes	
T1 Myocardial nulling before blood	Yes	No	Yes	Yes	-	No	Yes	Yes	Yes	Yes	Yes	
<b>Controls</b>												
	<b>1</b>			<b>2</b>			<b>3</b>			<b>4</b>		
Age (year)	68			63			69			61		
Sex	F			M			M			M		
Ethnicity	C			C			C			C		
BMI (kg/m <sup>2</sup> )	26.3			33.8			42.1			34.4		
NYHA class	2			1			4			3		
Diagnosis	HCM			HCM			ICMP			ICMP		
Comorbidities												
HTA	No			Yes			Yes			Yes		
DLP	No			No			Yes			Yes		

**Table 1.** continued

	<b>Controls</b>			
	<b>1</b>	<b>2</b>	<b>3</b>	<b>4</b>
CAD	No	No	Yes	Yes
Diabetes	No	Yes	Yes	Yes
Laboratories				
Troponin (ng/L)	-	16	25	13
NTproBNP (ng/L)	-	832	962	428
Calcium (mmol/L)	2.28	-	-	2.28
Creatinine (μmol/L)	90	58	140	57
eGFR (mL/min/1.73m <sup>2</sup> )	57	> 60	44	> 60
Kappa (mg/L)	42.4	48.1	-	44.2
Lambda (mg/L)	86.2	21.4	-	-
Kappa:Lambda Ratio	10.8	15.7	-	-
ECG				
Low Voltage	No	No	PMP	No
LVH	Yes	Yes	PMP	No
QRS (ms)	94	90	PMP	100
Echo				
LVEF (%)	65	65	55	50
LV mass (g/m <sup>2</sup> )	69	129	11	126
Septum width (mm)	11	18	13	12
E/e'	-	-	14	-
Global strain (%)	-	- 13.6	-	-
cMRI				
LGE	yes	no	-	-
Heterogeneous T1 nulling	no	no	-	-
T1 Myocardial nulling before blood	no	no	-	-

\*Subjects with false-negative <sup>18</sup>F-NaF PET/CT

## RESULTS

### Study Cohort

The demographic, clinical, and imaging characteristics of the subjects with CA and control cases are presented in Table 1. The study cohort consisted of 7 subjects with ATTR, four with AL, and four controls. Genetic testing was performed in three subjects with ATTR and no TTR mutations were identified. The diagnosis of CA was confirmed by biopsy in all four AL subjects. For subjects with ATTR, the diagnosis was confirmed by EMB in three cases, while, for the remaining four subjects, the diagnosis was confirmed by positive bone scintigraphy with the absence of light-chain level abnormalities on SPEP. Two control subjects had a hypertrophic cardiomyopathy and two had an ischemic cardiomyopathy.

### Subjective Interpretation

Consensus qualitative, gestalt interpretation resulted in four true-positive and three false-negative studies in those subjects with ATTR. Characteristics of subjects with false-negative studies are presented in Table 1. All four studies of the subjects with AL as well as the four controls were correctly interpreted as negative. Qualitative interpretation yielded a sensitivity of 57% (95% CI 18-90%) and a specificity of 100% (95% CI 63-100%) for the detection of ATTR. For the three false-negative studies in subjects with ATTR, the final diagnosis was established by EMB. In one subject with false-negative <sup>18</sup>F-NaF PET/CT (ATTR subject #7), the study was interpreted as negative by both readers; however, an EMB confirmed the diagnosis of ATTR and a PYP study showed greater intense uptake than that surrounding bone structures corresponding to grade-3 uptake<sup>10</sup> on 3-hour planar and SPECT images, with a heart-to-background ratio of 1.9 on planar 1-hour images (Figure 2).

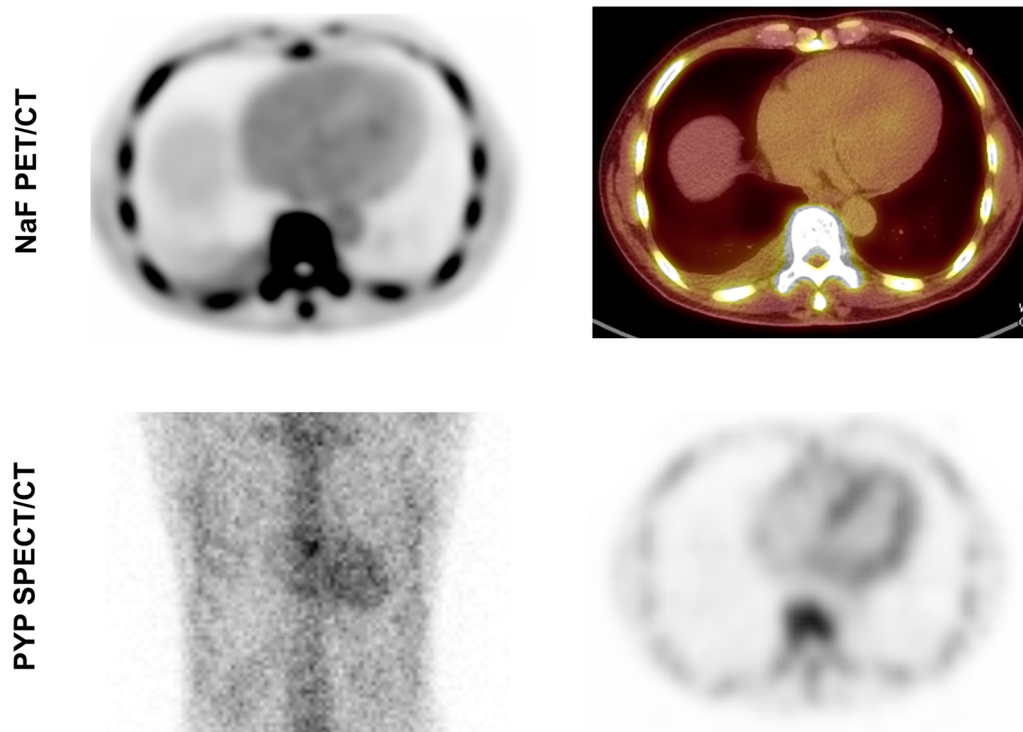


**Figure 2.**  $^{18}\text{F}$ -NaF PET/CT study (top) of a patient with biopsy-confirmed ATTR. The  $^{18}\text{F}$ -NaF PET/CT study was interpreted as negative by both readers. Myocardial uptake is below surrounding blood pool activity with a  $\text{TBR}_{\text{mean}}$  of 0.93. A PYP-SPECT study revealed Grade 3 uptake on the 3-hour planar and SPECT images (bottom).

The interreader agreement was very good with a  $\kappa = 0.84$  (95%CI: 0.55-1.00). In one case only did the readers' interpretation differed. After consensus interpretation, the study (of a subject with biopsy-proven AL) was correctly interpreted as negative for ATTR.

### Quantitative Interpretation

The average SUV over the entire LV ( $\text{SUV}_{\text{mean}}$ ) did not differ significantly (Figure 3,  $P = .14$ ) in ATTR subjects ( $1.31 \pm 0.30$ ) when compared to AL subjects ( $0.84 \pm 0.55$ ) or controls ( $1.29 \pm 0.21$ ). On the other hand, average LV  $\text{TBR}_{\text{mean}}$  was significantly greater (Figure 3) in ATTR subjects ( $0.98 \pm 0.09$ ) compared to both AL ( $0.85 \pm 0.08$ ,  $P = .026$ ) and control ( $0.82 \pm 0.07$ ,  $P = .020$ ) subjects. In four (57%) ATTR subjects,  $\text{TBR}_{\text{mean}}$  was inferior to 1.0, indicating LV uptake inferior to blood pool activity.  $\text{TBR}_{\text{mean}}$  remained essentially stable between 60 and 90 min post tracer injection in all the three groups (Figure 4). The average  $\text{TBR}_{\text{mean}}$  of the 17 LV segments is presented in Figure 5. In ATTR subjects, the basal segments showed increased  $\text{TBR}_{\text{mean}}$  compared to the mid and apical

segments, while uptake values in the subjects with AL and the controls were more homogeneous.

ROC analysis of  $\text{TBR}_{\text{mean}}$  yielded an AUC of  $0.91 \pm 0.08$  ( $P = .0078$ ) with optimal sensitivity and specificity of 75% (95%CI: 35-97%) and 100% (95%CI: 59-100%) using a cutoff  $\text{TBR}_{\text{mean}}$  value of 0.89 for the diagnosis of ATTR. ROC analysis of  $\text{SUV}_{\text{mean}}$  yielded an AUC of  $0.66 \pm 0.14$  ( $P = .30$ ). The difference between  $\text{TBR}_{\text{mean}}$  and  $\text{SUV}_{\text{mean}}$  AUC did not reach statistical significance ( $P = .12$ ).

### Rest Perfusion Imaging

Rest perfusion imaging was performed with  $^{82}\text{Rb}$  PET/CT in 6 (86%) ATTR subjects, 4 (100%) AL subjects, and 3 (75%) control subjects, and  $^{99\text{m}}\text{Tc}$ -tetrofosmin SPECT/CT was performed in the remaining subjects. For those who underwent  $^{82}\text{Rb}$  PET/CT rest perfusion imaging, rest MBF values, in mL/min/g, were not significantly different ( $P = .11$ ) between ATTR ( $0.57 \pm 0.05$ ), AL ( $0.68 \pm 0.13$ ), and control subjects ( $0.80 \pm 0.26$ ).

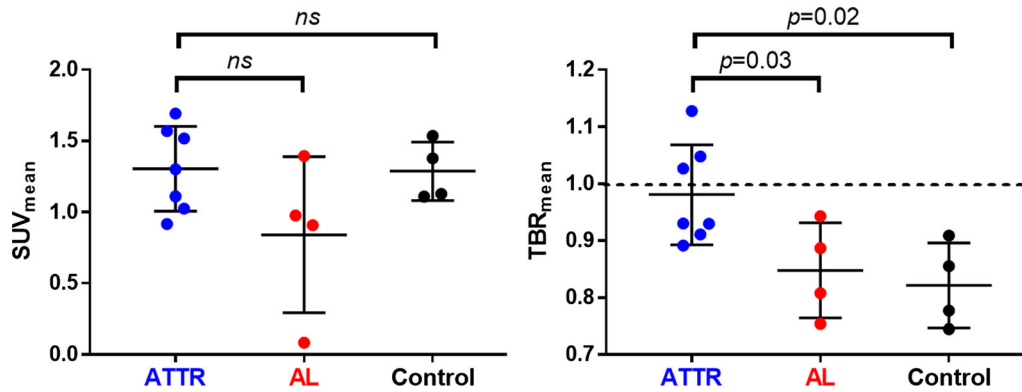


**Figure 3.** Comparison of the  $SUV_{mean}$  (left) and  $TBR_{mean}$  (right) in ATTR, AL, and control subjects.

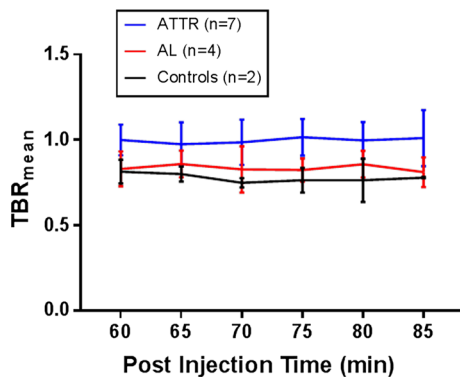


**Figure 4.** Target-to-background ratio ( $TBR_{mean}$ ) values over the acquisition time demonstrating significant overlap between the different groups of subjects, which persists throughout the entire acquisition time.

## DISCUSSION

The results of this study suggest that, while visual analysis of  $^{18}\text{F}$ -NaF PET/CT shows limited sensitivity in cases of ATTR, quantitative analysis results in moderate sensitivity. In comparison, our results show that gestalt interpretation of  $^{18}\text{F}$ -NaF PET/CT yielded a very low sensitivity but a very good interreader agreement. Furthermore, we found that  $TBR_{mean}$  was superior to  $SUV_{mean}$  for distinguishing ATTR from AL and controls.

Overall, the literature examining the use of  $^{18}\text{F}$ -NaF PET in subjects with CA is quite limited (Table 2). Although a case report described negative  $^{18}\text{F}$ -NaF PET in two subjects with ATTR,<sup>18</sup> two small prospective studies showed promising results. In 12 subjects, Morgenstern et al. showed that uptake in ATTR was significantly greater than in AL and controls.<sup>12</sup> Trivieri et al. obtained similar results in 14 subjects.<sup>13</sup> Of note, myocardial uptake values in both studies were relatively

mild, highlighting the importance of accurate quantitative assessment. In addition, the imaging protocols used in these studies varied, with acquisitions performed between 15 and 90 min post-IV injection (PIV).

Although the degree of myocardial  $^{18}\text{F}$ -NaF uptake is significantly greater in ATTR compared to AL and control subjects, the degree of uptake was quite modest and, in a majority of subjects (57%), inferior to that of blood pool. This is in striking contrast with PYP which has been shown to demonstrate intense myocardial uptake in ATTR, resulting in near-perfect sensitivity with high interreader agreement.<sup>8</sup> Moreover, there was significant overlap between the  $TBR_{mean}$  of subjects with ATTR and those with AL (Figure 3), limiting its ability to distinguish between the two subtypes of CA.

Similar to other studies using  $^{18}\text{F}$ -NaF PET/CT for the evaluation of CA,<sup>12,13</sup> the present study relied on  $SUV_{mean}$  and  $TBR_{mean}$  rather than  $SUV_{max}$  and  $TBR_{max}$ . We chose to perform quantitative analyses on mean values to avoid issues related to the intense uptake that can be encountered in the presence of valvular calcification, contamination from sternal uptake, and coronary calcifications. When these are present,  $^{18}\text{F}$ -NaF uptake can be very intense with uptake blooming into adjacent myocardium, leading to spurious quantification, and can result in an overestimation of the true myocardial uptake. Relying on mean values instead of maximum values can help minimize the impact of such contamination. This is especially critical given the very faint uptake observed in some ATTR subjects.

When using a quantitative approach, an optimal  $TBR_{mean}$  cutoff of 0.89 was obtained for the diagnosis of ATTR. This value is comparable with the  $TBR_{max}$  of 0.84 obtained in another recent study by Trivieri et al.<sup>13</sup> In both cases, the threshold value is clearly below nearby blood pool activity, emphasizing the importance of quantitative analysis. Indeed, when relying on

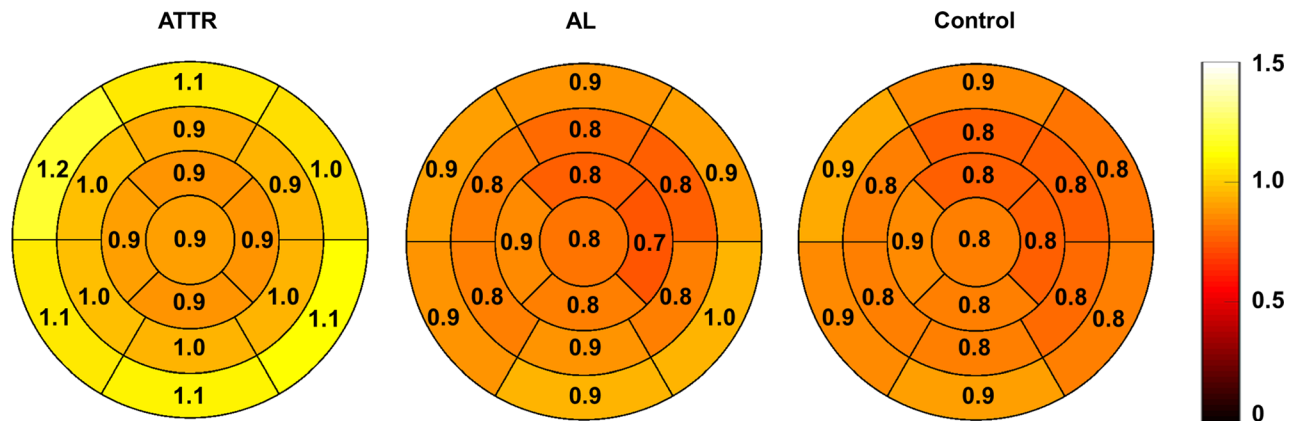


**Figure 5.** Average and TBR<sub>mean</sub> values of the 17 segments of the left ventricle for ATTR, AL, and control subjects.

quantitative analyses, the sensitivity of <sup>18</sup>F-NaF PET/CT improved from 57%, for visual interpretation alone, to a sensitivity of 75%. The very faint uptake seen in some ATTR subjects confirms the necessity of using quantitative analysis to support the interpretation of <sup>18</sup>F-NaF PET/CT studies as the distinction between degrees of uptake inferior to blood pool is exceedingly challenging without proper quantitative tools. Figure 2 illustrates an example for which both readers interpreted the study as negative for ATTR, while the quantitative analysis correctly classified the subject as positive for ATTR with a TBR<sub>mean</sub> of 0.93.

Interestingly, the distribution of <sup>18</sup>F-NaF uptake observed in ATTR subjects (Figure 5) shows a basal predominance with relative sparing of the apical and peri-apical segments. This distribution corresponds to a pattern also described on echocardiography where impaired LV longitudinal strain with apical sparing, the so-called cherry-on-sundae pattern, can be observed in patients with CA.<sup>19,20</sup>

In this study, SUV<sub>mean</sub>, as opposed to TBR<sub>mean</sub>, could not be used to discriminate between ATTR versus AL and control. This can likely be explained by the very low uptake seen in ATTR, which translated to low SUV values. Indeed, several technical and biological factors not related to the disease state are affecting SUV values, and when not correcting for blood pool activity, the amplitude of those variations is greater than the actual uptake related to CA.

In light of the results of this study, molecular imaging with PYP or DPD remains the imaging modality of choice to use in the investigation of ATTR, and in order to differentiate between ATTR and AL. Diagnostic performance is such that when using PYP and DPD imaging, diagnosis of CA can be confirmed without biopsy in significant proportion of subjects.<sup>8</sup> It is well

known that the diagnostic performances of SPECT bone-seeking radiopharmaceuticals are not all equal. For example, it has been shown that methylene diphosphonate (MDP) is less sensitive for the detection of ATTR compared to PYP.<sup>16</sup> Although different hypotheses have been proposed to explain the relatively low uptake of <sup>18</sup>F-NaF in ATTR compared to other bone tracers, the reasons for these differences in uptake between the various bone-seeking radiopharmaceuticals remain unclear. For example, it has been proposed that variable uptake intensity could be linked to the etiology of CA (mutant vs wild-type), to the stage of the disease (early vs late), or to the composition of the calcium matrix.<sup>21</sup> The results of this study suggest that <sup>18</sup>F-NaF PET/CT does not share the high sensitivity of PYP or DPD imaging and therefore may be of limited utility in the assessment of ATTR. Furthermore, whether a clearly positive <sup>18</sup>F-NaF PET/CT study in the absence of monoclonal gammopathy can be used to confirm the presence of ATTR has not been proven, and more studies are required to evaluate the diagnostic utility of this tracer, as well as to directly compare its accuracy with PYP or DPD.

The rest MBF values of ATTR subjects were on average inferior to the resting MBF values of AL and control subjects, but the difference did not reach statistical significance, likely related to the small sample size. This finding is in keeping with the results of another study demonstrating lower resting MBF in patients suffering from CA.<sup>22</sup>

This study suffered from several limitations. This was a retrospective study and was subject to the limitations of this study design, the overall number of subjects was also limited but is generally on par with other studies on CA imaging. An additional limitation was the fact that four ATTR subjects lacked biopsy confirmation of CA.



**Table 2.** Comparison of this study with other studies evaluating the role of <sup>18</sup>F-NaF PET/CT for the evaluation of cardiac amyloidosis

	<b>Martineau et al.</b>	<b>Morgenstern et al.</b> <sup>12</sup>	<b>Triviery et al.</b> <sup>13</sup>	<b>Gagliardi et al.</b> <sup>18</sup>	<b>Van Der Gucht et al.</b> <sup>14</sup>
Study design	Retrospective	Prospective	Prospective	Case report	Case Report
Sample size					
ATTRwt	7	3	2	1	0
ATTRm	0	2	2	1	1
AL	4	2	3	0	1
Controls	3	5	7	0	0
Total	14	12	14	2	2
Age years (SD)					
All	69 ± 11	71 ± 8	61 ± 12	-	-
ATTR subjects only	76 ± 7	67 ± 8	-	72 and 85	73
Male %	86	83	71	100	50
Acquisition protocol	Dynamic 60 to 90-min PIV PET/CT	Dynamic 10 to 60-min PIV PET/CT	Dynamic 20 to 90 min PIV PET/MR	15-min and 60-min PIV PET/CT	Early and 60-min PIV PET/CT
NaF	quantitative analysis	SUVmean and TBRmean	SUVmean	TBRmax	None
TBRmax					
Study findings	TBRmean is significantly greater in ATTR subjects (0.98) compared to AL (0.85) and control (0.82) subjects	SUVmean is significantly higher in ATTR (1.4) compared to controls (0.8)	TBRmax was significantly higher (1.14) in ATTR subjects compared to controls (0.68) and AL (0.77)	No significant uptakes in both subjects were seen on visual analysis	TBRmax was 1.4 in a ATTRm subject and 0.99 in a AL subject

AL, light-chain amyloidosis; ATTR, transthyretin amyloidosis; ATTRm, mutant ATTR; ATTRwt, wild-type ATTR; PIV, post-intravenous injection

For those subjects, the final diagnosis was established by the validated, noninvasive approach methods which rely on the presence of abnormal uptake on bone scintigraphy.<sup>8</sup> This introduces a bias which can lead to overestimation of the specificity and therefore the accuracy. Nonetheless, the main finding of this study is that the modest myocardial accumulation of <sup>18</sup>F-NaF in subjects with ATTR limits sensitivity.

### NEW KNOWLEDGE GAINED

The results of this pilot study suggest that the diagnostic sensitivity of <sup>18</sup>F-NaF for ATTR may be improved by making use of quantitative analysis; however, the overall sensitivity of the test remains inferior to the reported sensitivities of PYP and DPD SPECT.

### CONCLUSION

While <sup>18</sup>F-NaF PET/CT can discriminate between ATTR vs AL and controls, particularly when using quantitative analysis, it appears to be less sensitive than that established in nuclear medicine studies with PYP or DPD. Although <sup>18</sup>F-NaF PET/CT shows statistically higher TBR in ATTR compared to AL, the low TBR values observed in ATTR subjects (< 1.0) indicate poor myocardial signal, below that of blood pool activity. As such, <sup>18</sup>F-NaF PET is not yet ready for clinical use in CA, and further studies are needed to confirm its utility for the assessment of ATTR.

### Disclosures

*Patrick Martineau, Vincent Finnerty, Geneviève Giraldeau, Sébastien Authier, Francois Harel, and Matthieu Pelletier-Galarneau have nothing to disclose.*

### References

1. Maleszewski JJ. Cardiac amyloidosis: pathology, nomenclature, and typing. *Cardiovasc Pathol* 2015;24:343-50. <https://doi.org/10.1016/j.carpath.2015.07.008>.
2. Fikrle M, Paleček T, Kuchynka P, et al. Cardiac amyloidosis: A comprehensive review. *Cor et Vasa* 2013;55:e60-75. <https://doi.org/10.1016/j.crvasa.2012.11.018>.
3. Falk RH, Quarta CC, Dorbala S. How to image cardiac amyloidosis. *Circ Cardiovasc Imaging* 2014;7:552-62. <https://doi.org/10.1161/CIRCIMAGING.113.001396>.
4. Dharmarajan K, Maurer MS. Transthyretin cardiac amyloidosis in older North Americans. *J Am Geriatr Soc* 2012;60:765-74. <http://doi.org/10.1111/j.1532-5415.2011.03868.x>.
5. Bhogal S, Ladia V, Sitwala P, et al. Cardiac Amyloidosis: An Updated Review With Emphasis on Diagnosis and Future Directions. *Curr Probl Cardiol* 2018;43:10-34. <https://doi.org/10.1016/j.cpcardiol.2017.04.003>.
6. Maurer MS, Schwartz JH, Gundapaneni B, et al (2018) Tafamidis Treatment for Patients with Transthyretin Amyloid Cardiomyopathy. *N Engl J Med* <https://doi.org/10.1056/NEJMoa1805689>.
7. Adams D, Gonzalez-Duarte A, O'Riordan WD, et al. Patisiran, an RNAi Therapeutic, for Hereditary Transthyretin Amyloidosis. *N Engl J Med* 2018;379:11-21. <https://doi.org/10.1056/NEJMoa1716153>.
8. Gillmore JD, Maurer MS, Falk RH, et al. Nonbiopsy Diagnosis of Cardiac Transthyretin Amyloidosis. *Circulation* 2016;133:2404-12. <https://doi.org/10.1161/CIRCULATIONAHA.116.021612>.
9. Perugini E, Guidalotti PL, Salvi F, et al. Noninvasive Etiologic Diagnosis of Cardiac Amyloidosis Using <sup>99m</sup>Tc-3,3-Diphosphono-1,2-Propanodicarboxylic Acid Scintigraphy. *J Am Coll Cardiol* 2005;46:1076-84. <https://doi.org/10.1016/j.jacc.2005.05.073>.
10. Hutt DF, Quigley A-M, Page J, et al. Utility and limitations of 3,3-diphosphono-1,2-propanodicarboxylic acid scintigraphy in systemic amyloidosis. *Eur Heart J Cardiovasc Imaging* 2014;15:1289-98. <https://doi.org/10.1093/ehjci/jeu107>.
11. Bokhari S, Castaño A, Pozniakoff T, et al (2013) <sup>99m</sup>Tc-pyrophosphate scintigraphy for differentiating light-chain cardiac amyloidosis from the transthyretin-related familial and senile cardiac amyloidosis: clinical perspective. *Circulation* 6:195-201. <https://doi.org/10.1161/CIRCIMAGING.112.000132>.
12. Morgenstern R, Yeh R, Castano A, et al. 18 Fluorine sodium fluoride positron emission tomography, a potential biomarker of transthyretin cardiac amyloidosis. *J Nucl Cardiol* 2017;25:1-9.
13. Trivieri MG, Dweck MR, Abgral R, et al. 18F-sodium fluoride PET/MR for the assessment of cardiac amyloidosis. *J Am Coll Cardiol* 2016;68:2712-4.
14. Van Der Gucht A, Galat A, Rosso J, et al. [<sup>18</sup>F]-NaF PET/CT imaging in cardiac amyloidosis. *J Nucl Cardiol* 2016;23:846-9.
15. Gallegos C, Miller EJ. Use of fluorine-18 sodium fluoride for the diagnosis of transthyretin cardiac amyloidosis: The birth of a new technique. *J Nucl Cardiol* 2018;25:1568-70. <https://doi.org/10.1007/s12350-017-0847-6>.
16. Rapezzi C, Gagliardi C, Milandri A (2018) Analogies and disparities among scintigraphic bone tracers in the diagnosis of cardiac and non-cardiac ATTR amyloidosis. *J Nucl Cardiol* <http://doi.org/10.1007/s12350-018-1235-6>.
17. Lortie M, Beanlands RSB, Yoshinaga K, et al. Quantification of myocardial blood flow with <sup>82</sup>Rb dynamic PET imaging. *Eur J Nucl Med Mol Imaging* 2007;34:1765-74. <https://doi.org/10.1007/s00259-007-0478-2>.
18. Gagliardi C, Tabacchi E, Bonfiglioli R, et al. Does the etiology of cardiac amyloidosis determine the myocardial uptake of [<sup>18</sup>F]-NaF PET/CT? *J Nucl Cardiol* 2017;24:746-9.
19. Falk RH, Quarta CC. Echocardiography in cardiac amyloidosis. *Heart Fail Rev* 2015;20:125-31.
20. Phelan D, Collier P, Thavendiranathan P, et al. Relative apical sparing of longitudinal strain using two-dimensional speckle-tracking echocardiography is both sensitive and specific for the diagnosis of cardiac amyloidosis. *Heart* 2012;98:1442-8.
21. Ng QKT, Sethi P, Saunders TA, et al. Discordant Findings on 18F-NaF and <sup>99m</sup>Tc-HDP Bone Scans in a Patient With ATTR Cardiac Amyloidosis. *Clin Nucl Med* 2018;43:e89-92. <https://doi.org/10.1097/RLU.0000000000001933>.
22. Dorbala S, Vangala D, Bruyere J, et al. Coronary microvascular dysfunction is related to abnormalities in myocardial structure and function in cardiac amyloidosis. *JACC* 2014;2:358-67. <https://doi.org/10.1016/j.jchf.2014.03.009>.

**Publisher's Note** Springer Nature remains neutral with regard to jurisdictional claims in published maps and institutional affiliations.